

## EXPERIMENTAL AND MODELING INVESTIGATION OF THE EFFECT OF VENTILATION ON SMOKE ROLLBACK IN A MINE ENTRY

John C. Edwards, Robert A. Franks, Gene F. Friel, and Liming Yuan  
National Institute for Occupational Safety and Health  
Pittsburgh Research Laboratory, Pittsburgh, PA

### Abstract

Diesel fuel fire experiments were conducted in NIOSH's Pittsburgh Research Laboratory's (PRL) Safety Research Coal Mine (SRCM) to determine the critical air velocity for preventing smoke rollback. Such information is necessary for the preplanning and implementation of ventilation changes during mine fire fighting and rescue operations. The fire intensity varied from 50 kW to 300 kW depending upon the fuel tray area. Airflow in the 2 m high and 2.9 m wide coal mine entry was regulated during the course of each experiment; measured upwind from the fire as an average over the entry cross-section with an ultrasonic airflow sensor; and recorded dynamically with a mine monitoring system. The extent of smoke reversal was monitored with light obscuration monitors, ionization smoke sensors, and visual observations. Experimental results for the critical air velocity for smoke reversal as a function of fire intensity compared very well with model predictions based upon a computational fluid dynamics (CFD) fire dynamics simulator.

### Introduction

An underground mine fire can have devastating consequences for miners and the mine if not controlled in its incipient stage. Inhalation of the fire-generated toxic products-of-combustion (POC) can be injurious or fatal for miners, and the heat released can induce roof and rib collapses. Initially the thermal buoyancy forces generated by the fire will produce an ascending plume of fire POC. With sufficient ventilation, the POC will initially be transported downwind from the fire. Once the fire has evolved to sufficient intensity, the buoyancy forces will overcome the inertial forces of the ventilation, and the POC will migrate upwind along the roof counter to the positive ventilation. As noted by Mitchell [1], smoke from mine fires always rolls back in sufficiently low airflows, and can contain combustible gases, which are

subject to ignition by the mine fire when diluted by air. This poses a risk for the firefighters. The extent of smoke rollback along the roof into the fresh air will be determined by the ventilation velocity, airway dimensions, airway slope, and fire intensity. Moderately small quantities of fuel can generate significant heat and smoke. A diesel fuel spill covering a 0.93 m diameter circular area would generate a 1 MW fire. Similarly, a conical pile of broken coal with a 4.57 m diameter at the base, and a height of 1.83 m would generate a 1.5 MW fire. A wood crib 2.4 m high consisting of 1.22 m long timbers 0.15 m square can generate a 3.5 MW fire. The smoke layer above the fire will simultaneously thicken as the rollback occurs. Not only can the smoke prevent direct access to the fire, it can leak through stoppings into adjacent airways and thereby further endanger the miners. One extreme consequence of further increase in the fire intensity is that a sufficiently large heat production rate can produce flow reversal in an intake airway if the airway connects with parallel intake airways. The parallel airways could carry the balance of the airflow to maintain substantially the pre-fire mine pressure drop.

The use of ventilation to control the movement and dilution of smoke associated with an underground mine fire is recommended, but not quantified. Ventilation control, for example, is a recommended method [2] for the control of toxic products from shop areas in metal and nonmetal mines. However, a quantified ventilation strategy is not generally available for implementation. The primary reaction is egression from the mine fire region. Even under the best of circumstances the miners are often required to egress through a toxic low-visibility mine atmosphere produced by the mine fire. Similarly, any attempt to approach the fire from the intake side for its control and suppression will be thwarted by low visibility smoke conditions, and the toxic fire products, principally carbon monoxide (CO), associated with smoke backlayering. In the absence of remote real-time ventilation and POC monitoring, the selection of a ventilation change is not without unknown risks. To meet

the objective of establishing a safe procedure for ventilation induced smoke control, an experimental and a computational modeling approach was undertaken to determine the critical ventilation velocity required to prevent smoke reversal from fires of specific heat intensities. This information will be useful for preplanning and implementation of ventilation changes under emergency conditions. Experimental studies on smoke backlayering from a tunnel fire and determination of the critical velocity to prevent smoke backlayering have been conducted for a large tunnel [3] with a hydraulic diameter of 7.75 m, and small tunnels with hydraulic diameters between 0.18 m and 0.40 m [4]. Experiments in mine size tunnels with hydraulic diameter of 2.38 m were conducted at Buxton [4] with fire intensities greater than 200 kW. None of these cases were conducted in a mine entry, which with its rough walls introduces additional turbulence. This research considers fire intensities less than 300 kW in a coal mine entry for an evaluation of the critical velocity to prevent smoke reversal. The practical experimental limitations placed upon the conduct of experiments for large fire intensities necessitates the use of a predictive computational method to extrapolate limited experimental results to a range of fire intensities and mine entry dimensions not practically achievable experimentally. Modeling approaches can be semi-empirical analytic models, or field models which depend upon a numerical evaluation of the Navier-Stokes equations with a computational fluid dynamics (CFD) program. A one dimensional analytic model was developed by Kennedy [5] to investigate the critical ventilation velocity required to prevent smoke reversal. The model depends upon an estimate of the Froude number to prevent smoke reversal. Mitchell [1, p. A-2] has proposed a simple relationship for estimating the critical velocity for smoke rollback in relation to the entry height, but independent of fire intensity. Wu and Bakar [4] have used a field model to determine the dependence of the critical velocity upon fire intensity for laboratory scale tunnel fires. A CFD approach will also predict the length of the smoke backlayer for subcritical air velocities. The length of stationary smoke backlayer as a function of fire intensity and ventilation velocity has been modeled by Hwang and Edwards [6] with a CFD computer program.

### Experimental Procedure

The entry selected for the smoke reversal experiments was 126 m long, and had an average height of 2.06 m and width of 2.91 m, and was formed from a right angle bend with the intake portal. Figure 1 shows a plan view of the fire location and the doors used for

regulating the airflow. The fire was located 40 m downwind from the bend. At this distance the ratio of the airway length to hydraulic diameter was 17, which assures the turbulent flow velocity was uniform. Five-point vane anemometer measurements made over the entry cross-section at the fire zone indicated this to be the case. The slope of the airway upwind and downwind from the fire was less than 0.2 °, and was thereby inconsequential for smoke movement along the roof. The fire source on the entry floor consisted of a pan containing diesel fuel. To control the heat release rate, the fire pan surface areas ranged from 0.09 m<sup>2</sup> to 0.49 m<sup>2</sup> for the experiments. Monitoring of the smoke reversal was accomplished with two sensor stations located 3.05 m and 9.14 m upwind from the fire source, as well as markers spaced every 1.52 m upwind from the fire along the rib for visual observation. At each sensor station a light obscuration monitor was suspended approximately 0.5 m from the roof, above which was positioned an ionization smoke sensor. Approximately 4.6 m upwind from the fire source, near the roof and rib, was a transmitter-receiver of the ultrasonic air-flow measurement sensor. The other transmitter-receiver was located 8.28 m upwind on the entry's opposite rib near the floor. The acoustic airflow and smoke indication sensor outputs were sampled every two seconds by the mine monitoring system.

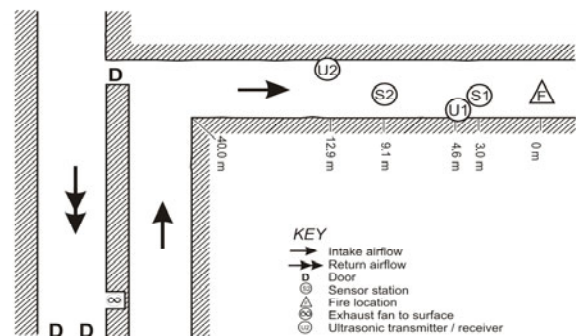


**Figure 1.** Plan view of mine test section

### Measurements

The fire effective tray size is listed in table 1 for each experiment. For each experiment the tray was centered on the entry floor relative to the ribs with the longer side positioned transverse to the entry. In experiments C, E, and F two trays were positioned adjacent to each other to form the effective tray area. The fire intensities and fuel mass fluxes were calculated from visual observation of the duration of flaming combustion for known fuel quantities, and the physical and chemical properties of the diesel fuel. The diesel fuel's mass density was 876 kg/m<sup>3</sup>,

and heat of combustion was 42.31 MJ/kg. Ignition was achieved by first pouring a small quantity (about 200 ml) of heptane on the diesel fuel. Prior to ignition, the airflow was measured with a vane anemometer at the fire tray. A five-point measurement was made at the airway center and corners. An average of these results was compared with the average acoustic measurement of the air velocity over the same time interval. For experiments A, B, and D the relative error was less than 1.2 %; for experiment C the relative error was 4.5%; for experiment E the relative error was 7.2%; and for experiment F the relative error was 3.6 %.

**Table 1. Fire pan size and interpolated fire intensity**

Exp	Effective Tray Size, m	Fuel, L	Fire Intensity Q, kW	Mass Flux, kg/s/m <sup>2</sup>
A	0.46 X 0.46	9.1	130	0.0147
B	0.61 X 0.61	15.1	267	0.017
C	1.07 X 0.46	20.8	304	0.0142
D	0.39 X 0.23	3.8	53	0.0155
E	0.79 X 0.23	7.6	102	0.0148
F	0.46 X 0.39	7.6	128	0.0187

Figure 2 shows the responses of the light monitor (LIGHT) and smoke sensor (SMOKE) 3.05 m upwind from the 130 kW fire for experiment A, and the response of the ultrasonic flow measurement instrument. The LIGHT and SMOKE values are normalized by their pre-fire ambient values. Also shown are several visually observed positions of the smoke roll back marked by the curve labeled EVENT. The extent of the smoke rollback is noted above the EVENT curve in figures 2 and 3. The light monitor, as an optical device, has a faster response to the presence of smoke particulates and their clearing, than the diffusion mode smoke sensor. From 9:04 AM to 9:08 AM the smoke was in the neighborhood of the sensors 3 m upwind from the fire pan. Instability in the roll back of the buoyancy-generated smoke resulted in significant fluctuations in the light and smoke sensor responses. Over this time period the ratio of the average signal to the signal's standard deviation was about 44 for the flow sensor, with reduced ratios of 11 for the light monitor and 3 for the smoke sensor. This illustrates how, for even a relatively steady airflow, the fire's fluctuating thermal effects will be amplified in the smoke movement. The ventilation velocity at the flow measurement device was 0.54 m/s when the smoke backlayer extended 6.1 to 9.1 m, 0.86 m/s when the backlayer extended 3.0 m, and 1.19 m / s when the smoke was maintained at the fire pan. These velocities are converted to average velocities at the fire pan based upon the 5.27 m<sup>2</sup> entry cross-sectional area

at the fire pan and 6.09 m<sup>2</sup> cross-sectional area at the flow monitor. The critical airflow at the fire pan for no smoke reversal is accordingly, 1.38 m/s. The restriction to human visibility posed by the smoke backlayer can be estimated from the output of the light obscuration monitor. At the reduced airflow of 0.63 m/s at the fire pan from 9:00 AM to 9:01:50 AM, which is a 54 % reduction in the ventilation velocity from its critical value, the average optical density of the smoke was 0.95 m<sup>-1</sup> and 0.31 m<sup>-1</sup> at the light monitors 3.05 m and 9.19 m upwind from the fire. These optical densities correspond to visibilities of 3.7 m and 11.3 m respectively based upon Jin's [7] relationship between visibility measured relative to a light emitting sign and the optical density. For a light reflecting sign the associated visibilities are 1.4 m and 4.2 m. Jin [7] also notes a minimum visibility of 3 m to 5 m is required for fire-escaping personnel familiar with the surroundings, and a visibility of 15 m to 20 m is required for personnel unfamiliar with the surroundings. Reliance upon a cap lamp's reflection from mine entry markings would be characteristic of reflection from a light reflecting sign. This shows the visibility limitation due to a relatively small 130 kW fire for someone familiar with the mine who, for mine escape, needs to rely upon a light from a cap lamp reflecting from mine entry markings.

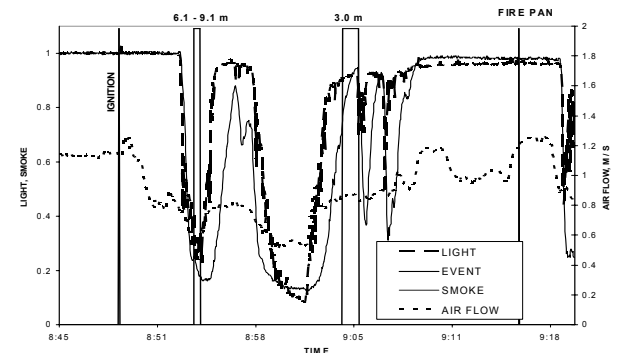


**Figure 2. Optical and smoke sensor dimensionless response at 3.05 m station, and airflow measurement for experiment A.**

Figure 3 shows similar results for the 304 kW fire of experiment C. The constant values for the measured airflow from 9:10 AM to 9:14 AM and from 9:28 AM to 9:34 AM are the result of very dense smoke which causes attenuation and refraction of the ultrasonic acoustic transmissions between the transmitter and receiver. For experiment C the ventilation velocity at the ultrasonic flow measurement device was 1.28 m / s when the smoke was stabilized at the fire pan. This corresponds to a 1.55 m / s flow velocity at the fire pan. A stationary roof smoke backlayer of 3 m developed for a ventilation of

0.97 m / s indicated by the flow measurement sensor, and a 4.3 m to 4.6 m backlayer developed for a ventilation of 0.93 m/s. Table 2 lists the critical velocity,  $V_c$ , at the fire pan to prevent smoke rollback for the six experiments. For the six experiments with fire intensity range from 53 kW to 304 kW, the ratio of the critical velocity to the velocity representative of a 3 m backlayer was 1.25, with a standard deviation of 0.10. It is instructive to represent the relationship between critical air velocity and fire intensity,  $Q$ , as dimensionless quantities. The dimensionless critical air velocity  $V_c^*$  and heat release rate  $Q^*$  are defined by the equations [4]:

$$V_c^* = V_c / \sqrt{gH} \quad (1)$$

$$Q^* = Q / (\rho_0 T_0 C_p \sqrt{gH^5}) \quad (2)$$

where  $\rho_0$  and  $T_0$  are the inlet ambient air density and temperature,  $C_p$  is the air specific heat (1.005 kJ/kg/K), and  $g$  is the acceleration due to gravity,  $9.8 \text{ m} / \text{s}^2$ . The characteristic length  $H$  is the hydraulic diameter of the entry. It is defined as four times the ratio of the entry cross sectional area to entry perimeter. For experiments C - F a thermal insulating material was attached to the roof at the fire location to protect the mine monitoring system data transmission cables from thermal damage. This reduction in the entry height at the fire pan accounts for variations shown for the hydraulic diameter,  $H$ , in table 2. Although these dimensionless variables account for the entry height and width through the hydraulic diameter, they do not account for the fire shape.

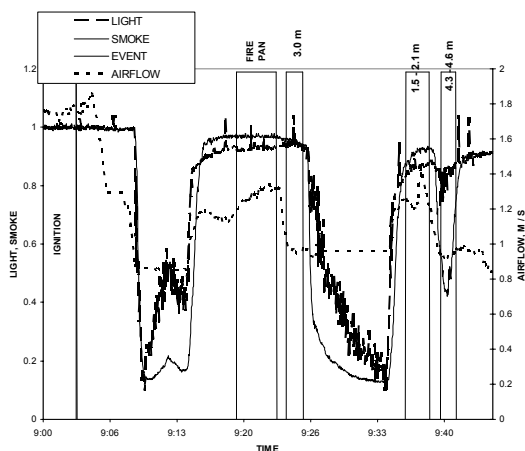


**Figure 3. Optical and smoke sensor response at 3.05 m station, and air flow measurement for experiment C.**

**Table 2. Mine fire critical velocity, and dimensionless critical velocity and fire intensity**

Exp	Fire Intensity, kW	$V_c$ , m/s	$H$ , m	$Q^*$	$V_c^*$
A	130	1.38	2.27	0.016	0.29
B	267	1.51	2.27	0.032	0.32
C	304	1.55	2.21	0.038	0.33
D	53	0.92	2.15	0.0070	0.20
E	102	1.08	2.15	0.0135	0.23
F	128	1.32	2.15	0.0171	0.29

Figure 4 shows the dependence of the dimensionless critical velocity upon the dimensionless heat release rate. The literature [3,8] shows a dependence of  $V_c$  upon  $Q$  to the one-third power. The trend line in figure 4 shows a power dependence equal to 0.30, which is in reasonable agreement with the theoretical  $1/3$  value. The R-Squared value, the square of the coefficient of correlation, was equal to 0.89. Shown for comparison are the dimensionless values reported for the experiments of Wu and Bakar [4], and the values they report for experiments conducted at Buxton over the comparable  $Q^*$  range from 0 to 0.04. The dimensionless critical velocities for the SRCM experiments are higher than the Buxton and Wu-Bakar values. Both the SRCM and Buxton experiments used a tunnel with comparable hydraulic diameters. For the Buxton gallery experiments the hydraulic diameter was 2.38 m, and for the SRCM experiments, the hydraulic value was 2.15 m, with thermal insulation at the roof, and 2.27 m without thermal insulation at the roof. A significant difference between the experiments was the arch-shaped roof of the Buxton tunnel, and the flat roof of the SRCM entry. Visual observations in the SRCM experiments indicated the visible flames did not fill the entry cross-section. The small tunnels used for the Wu and Bakar [4] experiments had hydraulic diameters between 0.25 m and 0.4 m. Wall roughness is a significant factor in the SRCM entry, whereas the other tunnels were smooth walled. The fire intensities associated with the kerosene fires in the Buxton gallery were between 0.3 and 20 MW, while those for the propane source fires in the Wu and Bakar experiments were between 1.4 and 28 kW. Another factor which contributes to the difference in the experiments is the geometry of the fire source.

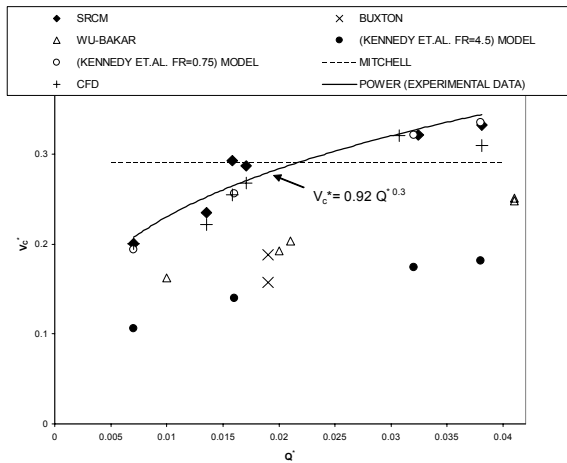


**Figure 4. Dimensionless critical velocity dependence upon dimensionless heat release rate**

Associated with smoke reversal is the roof layer's elevated temperature, which is characteristic of the smoke's buoyancy. For experiment E, the 102 kW fire, when the smoke had stabilized 12.2 m upwind from the fire, the smoke temperature at the roof was 66 °C above the fire, and 59 and 54 °C respectively 1.52 m and 3.05 m upwind from the fire. For experiment F, the 128 kW fire, when the smoke had stabilized 7.62 m upwind from the fire, the smoke temperature near the roof was 80 °C above the fire, and 61 and 58 °C respectively 1.52 m and 3.05 m upwind from the fire. At a location 10.2 m downwind from the fire the air temperature near the roof was 41 °C. The ambient temperatures were 22 and 20°C for experiments E and F respectively. This corresponds to Thomas's [8] observation that reverse flow is associated with hot smoke, and not cold smoke. This condition can be quantified by the Froude number. The Froude number  $Fr$  is defined as

$$Fr = g h (1 - T / T_f) / V^2 \quad (3)$$

where  $T_f$  is the hot gas layer temperature,  $T$  is the ambient temperature in degrees K,  $h$  is the tunnel height,  $g$  is the gravitational acceleration, and  $V$  is the ventilation velocity. Application of mass and energy conservation equations with the Froude numbers equal to 4.5 by Kennedy et.al. [5] leads to the predicted values shown in figure 4 for critical velocity. The selection of Froude number equal to 4.5 was based upon scale-model tests in ducts by Lee et. al. [9-10]. The SRCM fire tests results are more realistically modeled with  $Fr = 0.75$ , as shown in figure 4.

Mitchell [1, p.A-2] presents a rule-of-thumb for the critical velocity to prevent smoke rollback. Expressed in units of fpm, the critical velocity is equal to  $100\sqrt{h}$ ,

where  $h$  is the entry height in units of ft. When converted to dimensionless units with the identification of the hydraulic diameter with the entry height, the expression is  $V_c^* = 0.29$ . This value is independent of the heat release rate, and is shown as a constant value curve in figure 4. For  $Q^*$  values less than 0.022, the Mitchell estimate provides adequate ventilation for the prevention of smoke rollback for the SRCM fires. For  $Q^*$  values greater than 0.022, the Mitchell result underestimates the required ventilation for the prevention of smoke rollback. A  $Q^*$  value equal to 0.022 corresponds to a 135 kW fire for an entry with a 2 m hydraulic diameter.

## Modeling

NIST [11] has developed a CFD model of fire-driven fluid flow. NIST'S Fire Dynamics Simulator (FDS) is a numerical simulator for low Mach number flows with special applications to heat and smoke transport. The program solves the Navier-Stokes equations numerically for fluid flow with a mixture fraction combustion model. A significant feature of the program is the large scale eddy simulation (LES) method for turbulence. FDS was applied to a simulation of the six fire experiments conducted in the SRCM at PRL. The dimensions for the fuel tray and entry average cross-section were entered in detail. A 50 m length of tunnel section was used in the simulation with the fire located 30 m downwind from the entrance. The critical velocity for the experiment is determined from the analysis of the airflow at the roof. When the airflow at the roof does not extend upwind from the leading edge of the fire source, the inlet flow is at the critical velocity. For these computations a twenty second time average over the last twenty seconds of a five minute time interval was used to define the stationary state. These values were determined to be close to two minute time interval computations. Figure 4 shows good agreement between the SRCM experimentally determined critical velocity and the CFD predictions with FDS.

Although the instability of the smoke reversal made it difficult to define with great certainty the extent of smoke reversal for different ventilation velocities, a reduction of the data with dimensionless variables makes the trend more apparent. For the smoke reversal length  $L$  achieved for different ventilation velocities  $V_{in}$  and heat release rates  $Q$ , a pair of dimensionless variables,  $X$  and  $Y$ , can be defined as

$$X = Q / (A V_{in}^3 \rho_0) \text{ and} \quad (4)$$

$$Y = \frac{L}{H C_p (T_f - T_0)} \frac{gH}{gH} \quad (5)$$

where  $T_f$  is the flame temperature in degrees K. Figure 5 shows the parameters  $X$  and  $Y$  for the available experimental data. For this evaluation the flame temperature was set to 1,600 K. The correlation between  $X$  and  $Y$  satisfies the simple relationship  $Y=0.0238 \ln(X) - 0.0479$  with a R-Squared value, the square of the coefficient of correlation, equal to 0.68. The constant coefficients will change inversely with the selected flame temperature. The clustering of the data for the six different fire intensities near  $X = 11$ , in the range 7.8 to 14.1 for  $L=0$ , is representative of the approximate one-third power law dependence of the critical velocity upon the fire intensity noted above.

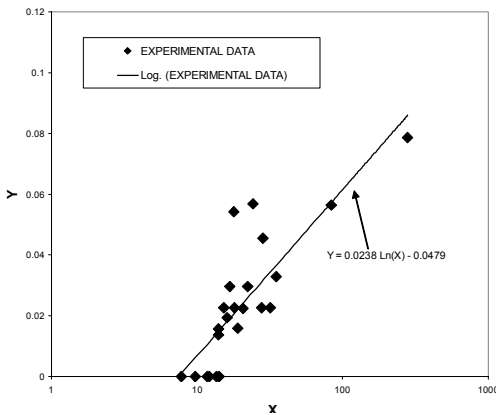


**Figure 5. Dimensionless correlation of smoke reversal length with fire intensity**

### Conclusions

It was demonstrated with fire smoke reversal experiments in the NIOSH SRCM that for a range of fire intensities between 50 and 300 kW in a mine entry 2 m high and 2.9 m wide that the critical velocity for preventing the development of a smoke layer upwind from the fire is proportional to the fire intensity to the 0.30 power. This is in substantial agreement with other researchers who posit a one-third law dependence upon the fire intensity. The development of visibility obscuration 9 m upwind from a small 130 kW fire when the ventilation velocity was reduced by 54% from its critical value demonstrated the importance for maintaining the critical ventilation velocity for smoke control. For the fires considered, the results are in approximate agreement with an empirical result which is independent of fire intensity. CFD modeling of the

dependence of the critical air velocity upon fire intensity showed good agreement with measured values.

### References

1. Mitchell, DW (1996), "Mine Fires Prevention, Detection, Fighting," (Intertec Publishing Inc, Chicago, IL), pp.19-20
2. Code of Federal Regulations, 30CFR, Part 57.4761. Office of the Federal Register, National Archives and Standards Administration, U.S. Government Printing Office, Washington, D.C., July 1, 2002.
3. Massachusetts Highway Department, (Boston, Mass), "Memorial Tunnel Fire Ventilation Test Program, Test Report", 1995
4. Wu Y and Bakar, M.Z.A. (2000), "Control of Smoke Flow in Tunnel Fires Using Longitudinal Ventilation Systems—A Study of the Critical Velocity", Fire Safety Journal, vol. 35, pp.363-390
5. Kennedy, WD, Gonzales, JA, and Sanchez, JG, (1996), "Derivation and Application of the SES Critical Velocity Equations", ASHRAE Transactions: Research, vol. 102, no.2, pp.40-44
6. Hwang, CC and Edwards, JC, (2001), "CFD Modeling of Smoke Reversal "Proceedings of the International Conference on Engineering Fire Protection Design" (Society of Fire Protection Engineers, Bethesda, MD) pp.376-387
7. Jin, T (1977), "Visibility through Fire Smoke", J. of Fire & Flammability, vol.9, pp. 135-155.
8. Thomas, PH (1970), "Movement of Smoke in Horizontal Corridors against an Airflow" Inst. Fire Engrs. Q. vol. 30, pp.45-53.
9. Lee, CK, Chaiken, RF, and Singer, JM (1979), "Interaction between Duct Fires and Ventilation: An Experimental Study" Combustion Science and Technology vol. 20, pp.59-72
10. Lee, CK, Hwang, CC, Singer, JM, and Chaiken, RF (1979), "Influence of Passageway Fires on Ventilation Flows" Second International Mine Ventilation Congress, Reno, NV
11. McGrattan, KB, Forney, GP, Prasad, KFloyd, JE, and Hostikka, S. (2002), "Fire Dynamics Simulator (Version3)-User's Guide", U.S. Dept. of Commerce, National Institute of Standards and Technology.